

Numerical modeling of nonneutral plasmas

Ross L. Spencer

Citation: [AIP Conference Proceedings](#) **331**, 204 (1995); doi: 10.1063/1.47894

View online: <http://dx.doi.org/10.1063/1.47894>

View Table of Contents:

<http://scitation.aip.org/content/aip/proceeding/aipcp/331?ver=pdfcov>

Published by the [AIP Publishing](#)

Articles you may be interested in

[Low-dimensional model of resistive interchange convection in magnetized plasma](#)

[AIP Conf. Proc.](#) **414**, 175 (1997); 10.1063/1.54444

[Vibration of moderately thick cylindrical shallow shells](#)

[J. Acoust. Soc. Am.](#) **100**, 3665 (1996); 10.1121/1.417229

[Electrostatic normal modes in nonneutral plasmas](#)

[AIP Conf. Proc.](#) **331**, 7 (1995); 10.1063/1.47907

[Thermal equilibrium properties of nonneutral plasma in the weak coupling approximation](#)

[AIP Conf. Proc.](#) **314**, 1 (1994); 10.1063/1.46751

[Role of ICRF induced ponderomotive force on the tokamak edge plasma](#)

[AIP Conf. Proc.](#) **159**, 334 (1987); 10.1063/1.36628

Numerical Modeling of Non-Neutral Plasmas

Ross L. Spencer

Department of Physics and Astronomy

Brigham Young University

Provo, Utah 84602

Several numerical tools for modeling non-neutral plasmas have been developed at Brigham Young University, including codes for computing equilibria, for simulating plasmas, and for computing mode frequencies with numerical eigenvalue methods. Our hope is that these programs will allow us to make careful comparisons between theory and experiment and allow us also to investigate the differences between various plasma models. This talk will summarize this work and give examples of physical applications.

I. INTRODUCTION

Non-neutral plasma experiments are performed in a wide variety of confinement geometries and on plasmas with widely varying parameters. As in the rest of plasma physics, it is unlikely that analytic theory alone will be capable of handling all of the interesting physics in these systems. Furthermore, plasma theory routinely produces equations that are practically impossible to solve, making it difficult to test the utility of our theoretical models. So it seems that the numerical work performed by various members of our community will continue to be important to the future of non-neutral plasma physics.

Our plasma theory group has developed, and is continuing to develop, codes that can be used to study non-neutral plasmas. Among the codes that have been developed are the following: (a) a general purpose axisymmetric equilibrium code, (b) an axisymmetric (rz) particle-in-cell simulation, (c) an $r\theta$ simulation for studying $\mathbf{E} \times \mathbf{B}$ drift dynamics, and (d) an eigenvalue code that finds linear mode frequencies for two-dimensional (rz) equilibria with perturbations proportional to $\exp(im\theta)$. In the remainder of this talk these codes will be briefly described and examples of their application to physical problems will be given.

II. EQUILIBRIUM

The equilibrium code that we have developed uses Successive-Over-Relaxation to solve non-linear Poisson equations of the form

$$\nabla^2 \phi = -\frac{q}{\epsilon_0} n(r, \phi) \quad (1)$$

in cylindrical geometry.¹ The boundary conditions can be specified in a variety of ways, including confining rings of arbitrary length and location as well as internal conducting structures of any shape (so long as they are axisymmetric). It also computes equilibria in three different ways. (1) It computes global thermal equilibria, in which both the radial and axial density profiles are self-consistently determined.² (2) It computes equilibria with a specified midplane radial profile. And (3), it computes equilibria whose line-density profile $h(r) = \int n(r, z) dz$ is specified, as would be appropriate for analyzing experiments where the plasma is diagnosed by dumping it onto charge collectors at the end of the confinement region.

As an example, Fig. 1 shows contours of constant density and electrostatic potential for a plasma equilibrium that matches a measured line-density profile in the positron trap experiments of Surko, Greaves, and Tinkle at the University of California at San Diego.³

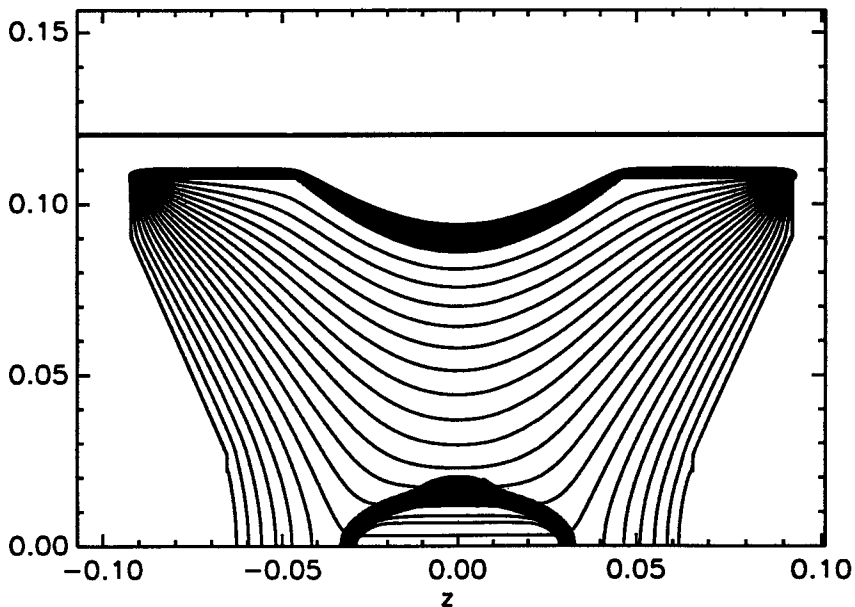


FIG. 1. Contours of constant density (clustered in the center) and constant electrostatic potential for a computed equilibrium whose line-density profile matches an experimentally measured profile.

III. SIMULATIONS

Two types of two-dimensional simulations have been developed for use with non-neutral plasmas: $r\theta$ simulations for infinitely-long plasmas, and an rz simulation for finite-length axisymmetric plasmas. Only the latter will be discussed here.

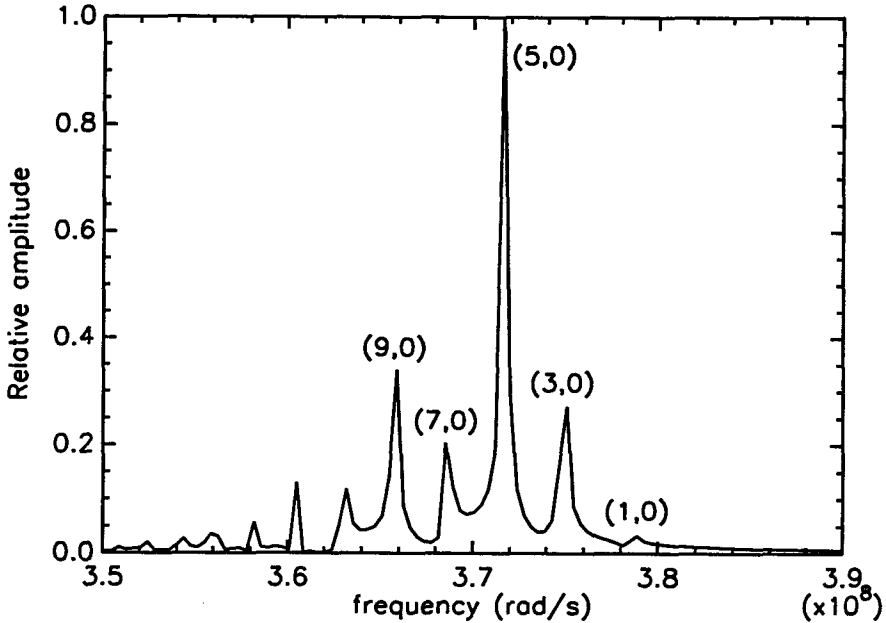


FIG. 2. Spectrum obtained from an rz simulation of “drumhead” modes in a pancake-like plasma in the geometry of the experiments of Weimer, et. al., at the National Institute of Science and Technology at Boulder. The peaks are labeled with their (ℓ, m) designations in Dubin’s notation; the initial perturbation for the run was based on Dubin’s eigenfunction for the $(5,0)$ mode.

The rz simulation is a particle-in-cell code, with the particles moving in a three-dimensional phase space (r, z, v_z) , although since the plasma is axisymmetric and drift motion is assumed in the plane perpendicular to the confining magnetic field, the r -positions of the particles never change once they are loaded. This code takes as input the geometry and plasma computed by the equilibrium code, after which perturbations are added to study various physical processes. This program simulated the axisymmetric vibrational motions of the plasmas produced in the positron trap experiments of Surko, Greaves, and Tinkle³ where it was used to study the possibility of using ratios between mode frequencies as a non-destructive diagnostic. The simulation was able to

give information about the variation of mode frequencies with temperature, functioning as a very sophisticated, but very slow, digital thermometer. This simulation has also been used to study the modes of vibration of the very thin pancake-like plasmas studied by Weimer, et. al., at the National Institute of Science and Technology at Boulder.⁴ By seeding the plasma with offsets in the z -direction appropriate to the modes calculated by Dubin for these plasmas⁵, the simulation can detect several of these modes in the real geometry of the experiment (to the extent that the experiment was axisymmetric, of course). Figure 2 shows the spectrum obtained from the simulation when a mode with $\ell = 5$ and $m = 0$ (Dubin's notation) was seeded. (The modes we can study are like the axisymmetric vibration modes of a drumhead.) The detection diagnostic picked up not only the mode that was seeded, but several neighboring modes as well, which gives a fortunate saving of computer time. This work is part of an ongoing study by Grant Mason on the suitability of mode frequency ratios in these pancake-like plasmas to measure their aspect ratios.

IV. EIGENVALUE CALCULATION

Simulations are a nice tool, but, like experiments, they are sometimes hard to interpret. For instance, it is difficult to find mode eigenfunctions, and it can be tricky to properly identify the peaks that come from a spectrum like that given in Fig. 2. The best thing is to be able to compare simulations with other kinds of theory, like perturbation analysis, to more fully explore the models used to describe plasmas.

To try to get a better theoretical description of the normal modes of non-neutral plasmas, and to explore the predictions of various models, we have begun to develop an eigenvalue code. Our hope is that we will be able to explore many different plasma models with this tool, but we have begun with a very simple one: the finite-temperature drift-fluid model. It assumes $\mathbf{E} \times \mathbf{B}$ drift motion perpendicular to the confining magnetic field and an adiabatic fluid response parallel to the confining field. The fluid equations corresponding to this description are

$$\frac{\partial n}{\partial t} + \mathbf{v}_d \cdot \nabla n + \frac{\partial}{\partial z}(nv_z) = 0 \quad ; \quad \frac{\partial p}{\partial t} + \mathbf{v}_d \cdot \nabla p + v_z \frac{\partial p}{\partial z} = -\gamma p \frac{\partial v_z}{\partial z} \quad (2)$$

$$\mathbf{v}_d = \frac{-\nabla \phi \times \hat{z}}{B} \quad ; \quad Mn \left[\frac{\partial}{\partial t} v_z + \mathbf{v} \cdot \nabla v_z \right] = -qn \frac{\partial \phi}{\partial z} - \frac{\partial p}{\partial z} \quad , \quad (3)$$

where n is the particle density, \mathbf{v}_d is the drift velocity perpendicular to the magnetic field \mathbf{B} , v_z is the fluid velocity parallel to \mathbf{B} , ϕ is the electrostatic potential, M is the particle mass, q is the particle charge, p is the fluid pressure

give information about the variation of mode frequencies with temperature, functioning as a very sophisticated, but very slow, digital thermometer. This simulation has also been used to study the modes of vibration of the very thin pancake-like plasmas studied by Weimer, et. al., at the National Institute of Science and Technology at Boulder.⁴ By seeding the plasma with offsets in the z -direction appropriate to the modes calculated by Dubin for these plasmas⁵, the simulation can detect several of these modes in the real geometry of the experiment (to the extent that the experiment was axisymmetric, of course). Figure 2 shows the spectrum obtained from the simulation when a mode with $\ell = 5$ and $m = 0$ (Dubin's notation) was seeded. (The modes we can study are like the axisymmetric vibration modes of a drumhead.) The detection diagnostic picked up not only the mode that was seeded, but several neighboring modes as well, which gives a fortunate saving of computer time. This work is part of an ongoing study by Grant Mason on the suitability of mode frequency ratios in these pancake-like plasmas to measure their aspect ratios.

IV. EIGENVALUE CALCULATION

Simulations are a nice tool, but they are fairly crude. For instance, it is difficult to find mode eigenfunctions from simulations, and it can be tricky to properly identify the peaks that come from a spectrum like that given in Fig. 2. In fact, perhaps the best way to think about simulations is as well-diagnosed experiments in a world with simplified and controllable physical laws. Simulations can guide theory, but they are not theory.

To try to get a better theoretical description of the normal modes of non-neutral plasmas, and to explore the predictions of various models, we have begun to develop an eigenvalue code. Our hope is that we will be able to explore many different plasma models with this tool, but we have begun with a very simple one: the finite-temperature drift-fluid model. It assumes $\mathbf{E} \times \mathbf{B}$ drift motion perpendicular to the confining magnetic field and an adiabatic fluid response parallel to the confining field. The fluid equations corresponding to this description are

$$\frac{\partial n}{\partial t} + \mathbf{v}_d \cdot \nabla n + \frac{\partial}{\partial z}(nv_z) = 0 \quad ; \quad \frac{\partial p}{\partial t} + \mathbf{v}_d \cdot \nabla p + v_z \frac{\partial p}{\partial z} = -\gamma p \frac{\partial v_z}{\partial z} \quad (2)$$

$$\mathbf{v}_d = \frac{-\nabla \phi \times \hat{z}}{B} \quad ; \quad Mn \left[\frac{\partial}{\partial t} v_z + \mathbf{v} \cdot \nabla v_z \right] = -qn \frac{\partial \phi}{\partial z} - \frac{\partial p}{\partial z} \quad , \quad (3)$$

where n is the particle density, \mathbf{v}_d is the drift velocity perpendicular to the magnetic field \mathbf{B} , v_z is the fluid velocity parallel to \mathbf{B} , ϕ is the electrostatic potential, M is the particle mass, q is the particle charge, p is the fluid pressure

parallel to \mathbf{B} , and where γ is the adiabatic exponent, which we take to be 3 because the strong magnetic field limits the kinetic response of the plasma to just one dimension.

When these equations are linearized to describe small perturbations about a non-neutral plasma equilibrium described by unperturbed density $n_o = n_o(r, z)$ and unperturbed electrostatic potential $\phi_o = \phi_o(r, z)$ the following mode equation results (assuming perturbations proportional to $\exp(im\theta - i\omega t)$):

$$\begin{aligned} & \gamma\lambda_D^2 \frac{\partial}{\partial z} \left[V \frac{\partial}{\partial z} \nabla^2 \phi \right] + \gamma\lambda_D^2 \frac{\partial}{\partial z} \left[V \frac{\partial F_o}{\partial z} \nabla^2 \phi \right] - \\ & \frac{(\gamma-1)mv_{th}^2}{r\omega_c} \frac{\partial}{\partial z} \left[V \frac{\partial}{\partial z} \left(\frac{\partial n_o / \partial r}{n_{oo}(\omega - m\omega_o)} \phi \right) \right] - \frac{(\gamma-1)mv_{th}^2}{r\omega_c} \frac{\partial}{\partial z} \left[V \frac{\partial F_o}{\partial z} \frac{\phi}{(\omega - m\omega_o)} \right] + \\ & \frac{(\omega - m\omega_o)}{\omega_p^2} \nabla^2 \phi - \frac{\partial}{\partial z} \left[V \frac{n_o}{n_{oo}} \frac{\partial \phi}{\partial z} \right] - \frac{m \partial n_o / \partial r}{r\omega_c n_{oo}} \phi = 0 \quad , \quad (4) \end{aligned}$$

where λ_D is the Debye length obtained from the central density n_{oo} , kT is the temperature (assumed independent of r and z) in energy units, $F_o = q\phi_o/kT$, $v_{th} = \sqrt{kT/M}$ is the thermal speed, ω_c is the cyclotron frequency, and where $\omega_o = \omega_o(r, z) = v_d/r$ is the equilibrium-drift rotation frequency. The quantity V which appears throughout the equation is given by

$$V(r, z) = \left[\omega - m\omega_o + (\gamma - 1)v_{th}^2 \frac{\partial}{\partial z} \left(\frac{\partial F_o / \partial z}{(\omega - m\omega_o)} \right) \right]^{-1} \quad (5)$$

It is perhaps worth noting that this mode equation in infinitely-long geometry works very well, giving essentially the same dispersion relation as the corresponding kinetic-theory calculation until Landau damping becomes important. Note also that as the temperature approaches zero only the last three terms in Eq. (4) survive and V approaches unity, recovering the cold mode equation given by Prasad and O’Neil⁶.

We have so far only solved the mode equation for axisymmetric modes ($m = 0$). The solution method we use has been developed by Johnny Jennings and K. C. Hansen, and consists of replacing the homogeneous problem given in Eq. (4) with an inhomogeneous problem, and then looking for the values of ω for which the problem becomes singular, as described below. Equation (4), which is of the form

$$L(\omega)\phi = 0 \quad , \quad (6)$$

is made inhomogeneous by replacing the zero on the right hand side by some convenient function $\rho(r, z)$:

$$L(\omega)\phi = \rho(r, z) \quad (7)$$

The function ρ is chosen to be similar to the structure of the mode being sought, i.e., ρ has the same number of radial and axial nodes as the mode.

This removes the difficulty that the equation is homogeneous, tempting the computer always to return $\phi = 0$ as the solution, and also shades the solutions found by the computer toward the desired mode. The mode frequencies ω are simply determined by varying ω , solving Eq. (7), and finding the values of ω which make its solution infinite (or at least very large). This works because the eigenvalues of a matrix are the values that make it singular.

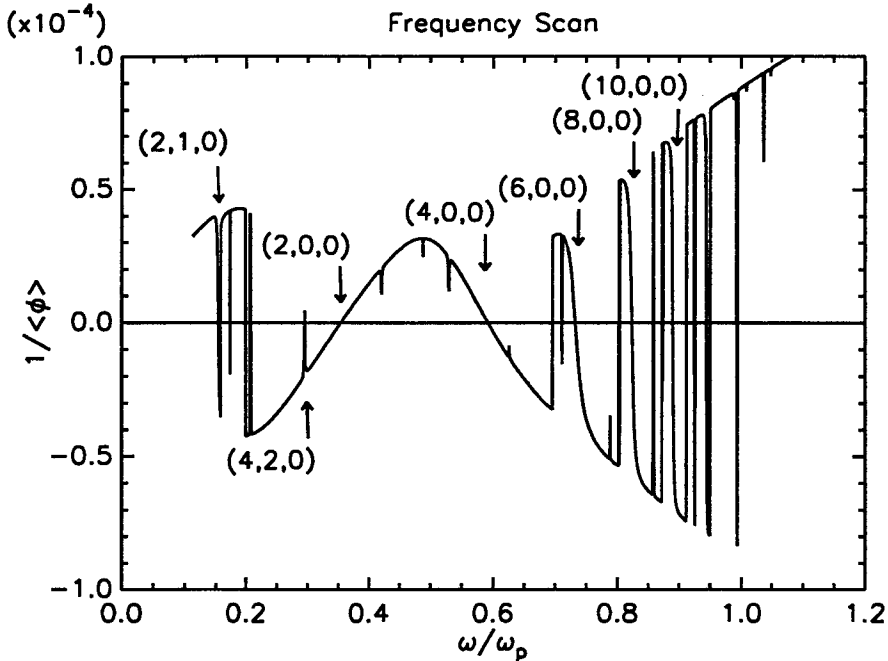


FIG. 3. The result of solving the finite-temperature mode equation for 1200 different values of ω and watching for singularities (zeroes of $1/\langle\phi\rangle$) where $\langle\phi\rangle$ is the volume average of the mode potential over the computing region. The labelling of the various modes follows the pattern (ℓ_z, ℓ_r, m) , where ℓ_z is the number of axial nodes along the cylinder axis and where ℓ_r is the number of radial nodes in the plasma midplane.

We use a finite-difference approximation to turn the operator $L(\omega)$ into a large square matrix with side-dimension equal to the number of points in the two-dimensional rz grid used to describe the plasma equilibrium. Fortunately the matrix is banded, but it is still huge, and because the system is nearly singular, the usual iterative solution methods that work so well for elliptic problems can't be used here. The best we have been able to do so far is just to use a banded system solver and use lots of memory. The memory required by the calculation on a grid with n_r radial points and n_z axial points is $n_r \times n_z \times (4n_r + 1) \times 8$ bytes (double precision). The calculations we have

done so far are limited by the 128 Mbytes of memory on our computer to grids of order 100×200 .

Figure 3 gives an example of this procedure of scanning the frequency and watching for singularities. The plasma equilibrium used is in a long cylinder with the radius of the plasma half as large as the cylinder radius and with the plasma half-length 5 times the plasma radius (the aspect ratio is 5). It is a global thermal equilibrium with a Debye length that is 6% of the plasma radius. The function ρ was chosen to have 2 axial nodes ($\ell_z = 2$) and no radial nodes ($\ell_r = 0$), corresponding to Dubin's ℓ -value having the value ($\ell = \ell_z + 2\ell_r = 2$). The mode identifications given in the figure are based on the appearance of the computed eigenfunction as a singular point is approached. As can be seen, the reciprocal of the volume-averaged mode potential $1/\langle \phi \rangle$ passes through zero several times, and one of these prominent zeroes corresponds to the (2,0) mode. Choosing the function ρ appropriately can make certain modes stand out, but the system will be singular near other modes as well, as can be seen in the figure. The modes sought don't always stand out as cleanly as the main ones do in Fig. 3, but they often do, making it possible sometimes to use zero-finding methods to find ω instead of scanning.

We have tested the eigenvalue code against other methods and typically find agreement to within 1-2%. For example, we have numerically computed the modes found analytically by Dubin (for the case of cold plasmas⁵) by analyzing several warm equilibria and extrapolating down to $T = 0$, and find agreement to about 1%. We have also compared with the experimental results and the simulations reported by Tinkle, et. al.³ Using the same equilibria employed in the simulations the eigenvalue code gives mode frequencies that are within 2% of the frequencies observed in the experiments.

A. Cold Cylindrical Plasmas

The eigenvalue calculation has been used to study the cold axisymmetric modes of non-neutral plasmas surrounded by cylindrical conducting walls. A similar calculation was done by Prasad and O'Neil, but without taking into account the correct equilibrium shape of the plasmas.⁶ We employed the technique of computing modes for several different temperatures, then extrapolating to $T = 0$. In all we performed about 400 singularity searches to find about 100 cold mode frequencies for various plasma radii, various plasma lengths, and for modes with $\ell_r = 0$ and $\ell_r = 1$. We find that for plasmas with lengths much shorter than the wall radius, Dubin's analysis⁵ gives accurate mode frequencies, i.e., image charge effects are unimportant for such plasmas. For plasmas whose lengths are about the same as the conducting wall radius, things are complicated and numerical calculations are probably required. But for plasmas whose lengths are longer than the wall radius, we find that a sim-

ple adjustment to the Trivelpiece-Gould dispersion relation for infinitely-long plasmas⁷ gives the same frequencies as the complicated numerical calculations to within 1%, or better. The Trivelpiece-Gould dispersion relation is obtained by assuming an infinitely long cold plasma with constant density so that the modes are proportional to $\exp(ikz)$, resulting in the relation

$$\frac{I'_o(kr_p)K_o(kr_w) - K'_o(kr_p)I_o(kr_w)}{I_o(kr_p)K_o(kr_w) - K_o(kr_p)I_o(kr_w)} = \beta \frac{J'_o(\beta kr_p)}{J_o(\beta kr_p)}, \quad (8)$$

where the I 's and K 's are modified Bessel functions, where r_p is the plasma radius, where r_w is the conducting wall radius, and where $\beta = \sqrt{\omega_p^2/\omega^2 - 1}$. Given a choice for k , this equation can be solved for the mode frequency ω . The adjustment uses the idea of an effective length for the plasma, similar to the use of an effective length for an open tube to accurately compute its resonant acoustic frequencies. To lowest order, there is a potential antinode at the end of the plasma,⁶ so the k of the mode is approximately

$$k = \frac{\pi \ell_z}{2z_p}, \quad (9)$$

where z_p is the half-length of the plasma. An analysis of the numerical results for modes with either $\ell_r = 0$ or $\ell_r = 1$ shows that the Trivelpiece-Gould dispersion relation can reproduce all of the numerical results for plasmas with $r_p/r_w = 0.25, 0.5, 0.75$ and with aspect ratios z_p/r_p greater than 3 if the formula for the wavenumber to use in Eq. (8) is modified by adding a simple correction to the plasma length, empirically determined from the numerical data:

$$k = \frac{\pi \ell_z}{2z_p + c_1 r_w + c_2 r_p}, \quad (10)$$

with

$$c_1 = 0.3 \quad ; \quad c_2 = 0.7 \quad \text{for } \ell_r = 0 \quad \text{and} \quad c_1 = -0.2 \quad ; \quad c_2 = 0.9 \quad \text{for } \ell_r = 1 \quad (11)$$

This makes it much easier accurately to compute mode frequencies for such plasmas, and future work will concentrate on trying to find similar simple connections to infinitely-long cylinder results when finite temperature and radial profile effects are included.

B. Acoustic Resonances

A natural calculation to perform with the eigenvalue code is the extension of Dubin's spheroidal study to finite temperature. To this end the equilibrium

and eigenvalue codes were modified to handle spheroids in infinite space and ω was scanned to look for modes. Figure 4 shows the result for a spherical plasma with the right-hand side of the mode equation chosen to look for the mode with $(\ell_r, \ell_z) = (2, 0)$. It looks like there should be a prominent mode near $0.9 \times 10^8 \text{ s}^{-1}$, but a bunch of extra modes seems to have gotten in the way.

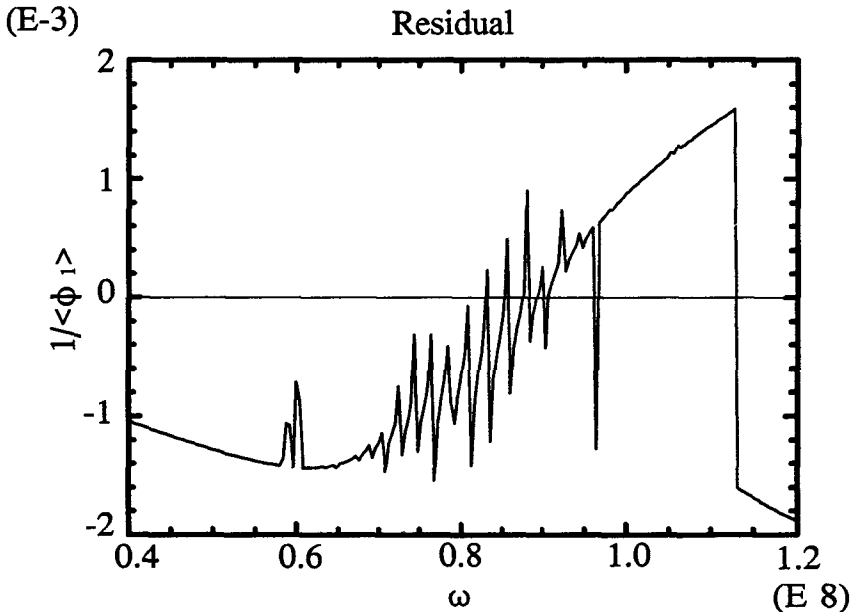


FIG. 4. The reciprocal of the volume-averaged potential vs. frequency is shown for a spheroidal plasma with aspect ratio 1 and a ratio of the Debye length to the plasma radius of 0.15. The mode being sought is the (2,0,0) mode, and its frequency at zero temperature is $0.775 \times 10^8 \text{ s}^{-1}$. The zig-zags in the middle are associated with continuum modes, and each would have appeared as a zero-crossing if a finer scan had been used.

If the grid resolution is doubled, the number of closely-spaced modes doubles, suggesting perhaps that the model has encountered a continuous spectrum which the grid is attempting to resolve by associating a mode with each grid point. This is, in fact, the case.

The continuous spectrum is connected with radii at which the mode frequency ω has a value for which the equation

$$\gamma \lambda_D^2 \frac{\partial}{\partial z} \left[V \frac{\partial}{\partial z} \nabla^2 \phi \right] + \gamma \lambda_D^2 \frac{\partial}{\partial z} \left[V \frac{\partial F_o}{\partial z} \nabla^2 \phi \right] - \frac{\omega}{\omega_p^2} \nabla^2 \phi = 0 \quad (12)$$

is satisfied for a non-trivial $\nabla^2\phi$. The terms in this equation are the terms from Eq. (4) containing the highest radial derivatives of the perturbed potential, and when this equation has a non-trivial solution at some radius, the mode equation is singular, similar to what happens in one-dimensional continuous spectrum problems when the coefficient of the highest derivative vanishes. The physical meaning of the singularity can be seen by taking the low-temperature limit, for which F_o is constant inside the plasma, transforming Eq. (12) into

$$\gamma \frac{kT}{M} \frac{\partial^2}{\partial z^2} \nabla^2 \phi + \nabla^2 \phi = 0 \quad , \quad (13)$$

the equation for one-dimensional sound waves. The continuum resonances occur roughly whenever

$$\omega = \sqrt{\frac{\gamma kT}{M} \frac{\pi \ell_z}{L(r)}} \quad , \quad (14)$$

where $L(r)$ is the plasma length at radius r . For rectangular plasmas $L(r)$ is nearly constant and doesn't interfere much with the electrostatic modes. But for spheroids, L approaches zero at the outer radius of the plasma, sweeping the acoustic resonances up through the modes of interest, as shown in Fig. 4, and ruining the mode calculation. This is an unphysical effect from the fluid model used in the calculation, for purely acoustic standing waves do not occur in one-component plasmas. This is a particularly striking case where the fluid theory simply gets it wrong, and to fix the calculation a better model (like kinetic theory or a non-local fluid theory) must be used. Future work will focus on using the solution techniques developed for the fluid problem to handle more complicated models.

¹ R. L. Spencer, S. N. Rasband, and Richard R. Vanfleet, *Phys. Fluids B* **5**, 4267 (1993).

² S. A. Prasad and T. M. O'Neil, *Phys. Fluids* **22**, 278 (1979).

³ M. D. Tinkle, R. D. Greaves, C. M. Surko, R. L. Spencer, and G. W. Mason, *Phys. Rev. Lett.* **72**, 352 (1994).

⁴ C. S. Weimer, J. J. Bollinger, F. L. Moore, and D. J. Wineland, *Phys. Rev. A*, **49**, 3842 (1994).

⁵ Daniel H. E. Dubin, *Phys. Rev. Lett.* **66**, 2076 (1991).

⁶ S. A. Prasad and T. M. O'Neil, *Phys. Fluids* **26**, 665 (1983).

⁷ A. W. Trivelpiece and R. W. Gould, *J. Plasma Physics* **30**, 1784 (1959).